NUCLEAR SCIENCE AND TECHNIQUES **25**, 040501 (2014)

An investigation on neutron induced reactions on stable CNO isotopes*

MA Chun-Wang (马春旺),[1,†] LÜ Cui-Juan (吕翠娟),[1] WEI Hui-Ling (魏慧玲),[1] and CAO Xi-Guang (曹喜光)[2]

[1] *Institute of Particle & Nuclear Physics, Henan Normal University, Xinxiang 453007, China*
[2] *Shanghai Institute of Applied Physics, Chinese Academy of Sciences, Shanghai 201800, China*

(Received April 24, 2014; accepted in revised form May 27, 2014; published online July 4, 2014)

The neutron induced reactions on stable Carbon, Nitrogen, and Oxygen isotopes are investigated by using the Talys1.4 toolkit with the default parameters. The neutron incident energy covers a range from 0.20 MeV to 85.00 MeV. For ^{12}C and ^{14}N, the Talys1.4 results agree with the experimental data, while the parameters should be adjusted for ^{16}O. Some $E_{\rm n}$ windows are found by comparing the main channels of n + C/N/O reactions, which induce element change. In these $E_{\rm n}$ windows, a specific element is activated to a different one while leaving the other element atoms unchanged. The results will facilitate the research of doping effects in organic materials by using neutron activation technique.

Keywords: Neutron activation, Doping, Organic material, C/N/O activation

DOI: 10.13538/j.1001-8042/nst.25.040501

I. INTRODUCTION

Doping is an important method to change the properties of materials. For example, the substitutions of some atoms in organic semi-conductors promote the charge transport and stability greatly [1, 2]. The general method for doping is chemical synthesis which introduces new elements into the original material. Actually, neutron activation is an important method to make doping in material, which can even change one element to other one, directly or after the decay of unstable isotopes produced by activation. In this situation, different to the chemical doping, different doping effects can be expected.

It is well known that for different nuclei, there are different threshold energy values for specific channels in neutron induced reactions [3]. For material having different elements, the different threshold energy values for neutron reactions provide a chance for specific activation if the neutron energy is selected in experiments.

In this article, the neutron induced reactions on stable carbon, nitrogen, and oxygen isotopes will be investigated by using a Talys toolkit. The energy windows between the different isotopes will be analyzed. The theory is briefly discussed in Sec. II. The results are discussed in Sec. III, and a summary is presented in Sec. IV.

II. METHODS

The optical model can describe the neutron induced reaction well in a wide range of incident energies. In Talys1.4, the ECIS-06 is implanted as a subroutine to deal with the optical model calculations [4]. The description of Talys1.4 and the implanted functions can be found in the user manual [5, 6].

In statistical models for predicting cross sections, nuclear level densities are used at excitation energies where discrete level information is not available or incomplete. Several models are implanted to describe the level density in Talys, which range from phenomenological analytical expressions to tabulated level densities derived from microscopic models. The constant temperature and Fermi-gas model is set as the default parameter of level density at low excitation energy region, while the Fermi-gas model is used in the high excitation energy region [6].

Due to the threshold energy exists for different channels in the neutron induced reaction on a nucleus, one channel can only happen if the incident energy of the neutron is above the threshold, which potentially provides energy windows only one channel can happen while the other channels are prohibited. In this work, the incident energy of the calculated reactions ranges from 0.20 MeV to 85.00 MeV, and the default parameters in Talys1.4 are adopted. The main reaction channels include (n, np), (n, p), (n, α), (n, 2n) and (n, γ). The calculated results are compared to the measured data, which are extracted from the EXFOR library provided by the National Nuclear Data Center (NNDC) [7]. All the natural abundance data and the half-life time of isotopes are taken from Wikipedia [8].

III. RESULTS AND DISCUSSION

A. Neutron induced reactions on carbon isotopes

The C element has two stable isotopes, ^{12}C and ^{13}C, with natural abundances of 98.93% and 1.07%, respectively. Only the n + ^{12,13}C reactions are calculated.

1. $n + {}^{12}C$ reactions

The ^{12}C(n, p)^{12}B, ^{12}C(n, α)^{9}Be, and ^{12}C(n, 2n)^{11}C channels have been measured previously. ^{12}B is an unstable nucleus, which decays to ^{12}C via electron emission with a half-

* Supported by the National Natural Science Foundation of China (No. 11305239), the Program for Science and Technology Innovation Talents in Universities of Henan Province (13HASTIT046)
† Corresponding author, machunwang@126.com

life time of 20.20 ms. ^{9}Be is a stable isotope. ^{11}C is also unstable, which decays to ^{11}B via positron emission with a relative long half-life time of 20.334 min. Thus the ^{12}C(n, 2n)^{11}C and ^{12}C(n, np)^{11}B channels are the main channels which result in element changes with the same final products, ^{11}B. The results are plotted in Fig. 1.

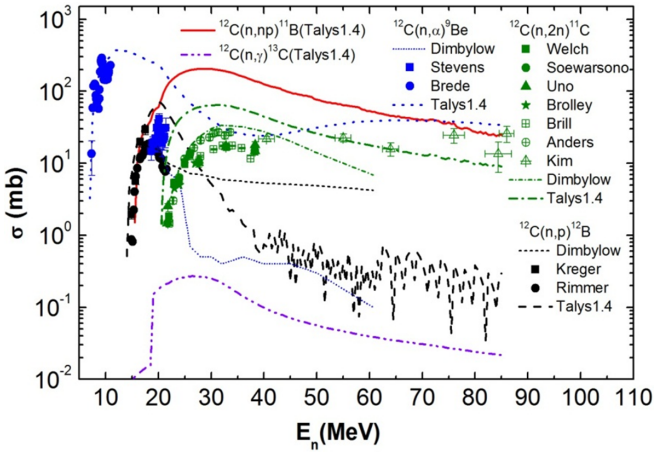

Fig. 1. (Color online) The yield of residues produced in n + ^{12}C reactions. The measured results are denoted by symbols, and the calculated results are represented by lines.

First, for the ^{12}C(n, α)^{9}Be channel, the Talys1.4 results are consistent with the measured results when E_n < 11.00 MeV [9], while the Talys1.4 results differ largely with the results measured by Stevens *et al.* [10] in the range of 18.65 MeV < E_n < 21.46 MeV. In the energy range of 20.00 MeV < E_n < 60.70 MeV, the Talys1.4 results are also much larger than the calculated results by Dimbylow *et al.* [11]. Above E_n > 11.00 MeV, the results of the ^{12}C(n, α)^{9}Be channel have large difference, which suggests that further experiment should be performed for a systematic understanding.

Second, for the ^{12}C(n, p)^{12}B channel, the measured results by Kreger *et al.* [12] and Rimmer *et al.* [13] coincide when E_n < 16.00 MeV, but differ when E_n is higher. The Talys1.4 results agree well with the measured results when E_n < 16.00 MeV, but overestimate the measured results by Kreger *et al.* [12] in the range of 16.00 MeV < E_n < 22.00 MeV. The calculated results of ^{12}C(n, p)^{12}B in the range of 20.00 MeV < E_n < 60.70 MeV by Dimbylow *et al.* [11], which also uses the optical model, prefer the measured results by Kreger *et al.* [12]. Meanwhile, the Talys1.4 predicts similar results between ^{12}C(n, p)^{12}B and ^{12}C(n, np)^{11}B reactions when E_n < 20.00 MeV.

Third, for the ^{12}C(n, 2n)^{11}C channel, which have been measured by many groups, the measured data agree well when E_n < 27.00 MeV. The results can be divided into two groups in the range of 27.00 MeV < E_n < 40.00 MeV, of which the upper group was measured by Welch *et al.* [14], Anders *et al.* [15], and Kim *et al.* [16]; and the bottom group by Brill *et al.* [17], Uno *et al.* [18], Brolley *et al.* [19], and Soewarsono *et al.* [20]. The calculated results by Dimbylow *et al.* [11] prefer the upper group results when E_n < 35.00 MeV. Kim *et al.* [16] measured the results in the energy range from 55.00 MeV to 64.00 MeV. The calculated results by Talys1.4 largely overestimate the measured ones when E_n < 50.00 MeV, but agree with the measured results by Kim *et al.* [16]. The calculated results by Dimbylow *et al.* [11] underestimate the measured results by Kim *et al.* [16].

The threshold energies of the ^{12}C(n, α)^{9}Be, ^{12}C(n, p)^{12}B, ^{12}C(n, np)^{11}B and ^{12}C(n, 2n)^{11}C channels increase, which are about 6.18 MeV, 13.64 MeV, 14.89 MeV and 20.30 MeV, respectively. The ^{12}C(n, γ)^{13}C channel happens in the whole energy range, but have a much smaller probability compared to other channels.

2. $n + {}^{13}C$ reactions

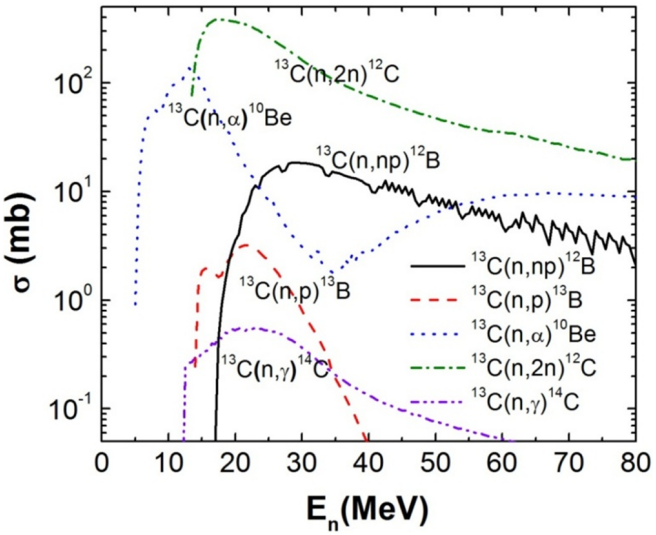

Fig. 2. (Color online) The yield of residues produced in the different channels of the n + ^{13}C reactions calculated by Talys1.4.

No measured data for the neutron induced reactions on ^{13}C is found. The Talys1.4 calculated results are plotted in Fig. 2. The threshold energy values increase with the (n, α), (n, 2n), (n, p) and (n, np) channels, with the values 4.13 MeV, 5.33 MeV, 13.64 MeV and 16.50 MeV, respectively. The (n, γ) channel has no lowest energy threshold. The (n, γ) and (n, p) channels have relatively low probabilities compared to the other channels. In the whole energy range calculated, when E_n < 15.00 MeV, the main channel is ^{13}C(n, α)^{10}Be, in which ^{10}Be decays to ^{10}B by electron emission with a very long half-life time 1.39 × 10^{6} years; when E_n > 15.00 MeV, the dominant channel is ^{13}C(n, np)^{12}B, in which ^{12}B mainly decays to ^{12}C with a half-life time 20.20 ms.

B. Neutron induced reactions on nitrogen isotopes

The N element has two stable isotopes, ^{14}N and ^{15}N, with a natural abundance of 99.64% and 0.36%, respectively. Only the n + ^{14,15}N reactions are calculated.

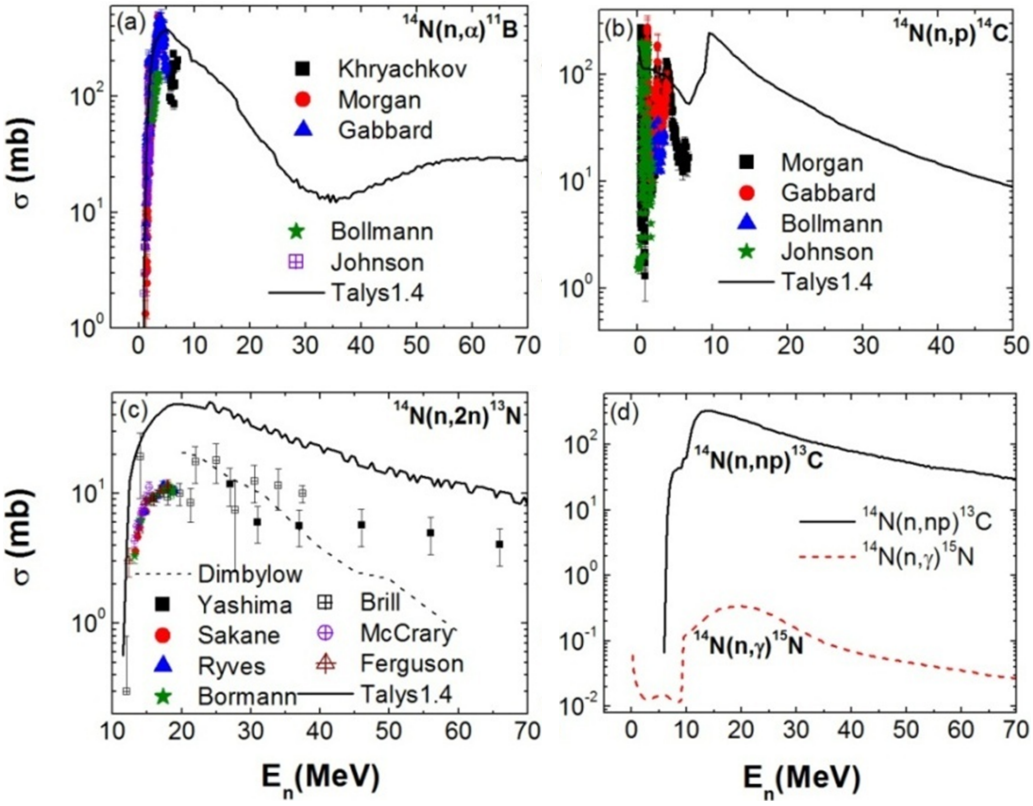

Fig. 3. (Color online) The yield of residues produced in the different channel of n + ^{14}N reactions: (a) ^{14}N(n, α)^{11}B; (b) ^{14}N(n, p)^{14}C; (c) ^{14}N(n, 2n)^{13}N; and (d) ^{14}N(n, np)^{13}C and ^{14}N(n, γ)^{15}N. The calculated results are plotted as different lines.

1. $n + {}^{14}N$ reactions

The calculated channels for the n + ^{14}N reaction are ^{14}N(n, np)^{13}C, ^{14}N(n, p)^{14}C, ^{14}N(n, α)^{11}B, ^{14}N(n, γ)^{15}N, and ^{14}N(n, 2n)^{13}N reactions, respectively. The nuclei ^{13}C, ^{15}N, and ^{11}B are stable, while ^{14}C and ^{13}N are unstable. ^{13}N decays to ^{13}C by positron emission with a half-life time 9.965 min. The (n, np), (n, p), (n, 2n), and (n, α) channels are the main ones which will result in element changes.

The results of the n + ^{14}N reaction are plotted in Fig. 3. For clarity, the results are plotted in different panels. The ^{14}N(n, α)^{11}B and ^{14}N(n, p)^{14}C have small threshold energies, which are very similar. The ^{14}N(n, α)^{11}B channel has been measured by different groups [21–25], and the ^{14}N(n, p)^{14}C has also been measured [21, 23–25]. For the two channels, the data measured by different groups is consistent. The Talys1.4 results agree with the measured data in the low incident energies, but overestimate the measured results when the E_n increases.

For the ^{14}N(n, 2n)^{13}N channel, the measured results [26–30] are consistent when $E_n < 19.00$ MeV. When $E_n > 24.00$ MeV, the measured results by Brill *et al.* [17] and Yashima *et al.* [31] are relatively consistent, and the calculated results by Dimbylow *et al.* [11] also agree with the measured data but have relatively large errors. The predicted threshold energy value by Talys1.4 is $E_n \approx 11.00$ MeV, but the Talys1.4 cross sections overestimate the measured results in the whole energy range, which increases fast with E_n and reaches maximum at $E_n = 24.00$ MeV and decreases with E_n when $E_n > 24.00$ MeV. Since ^{13}N decays to ^{13}C, the

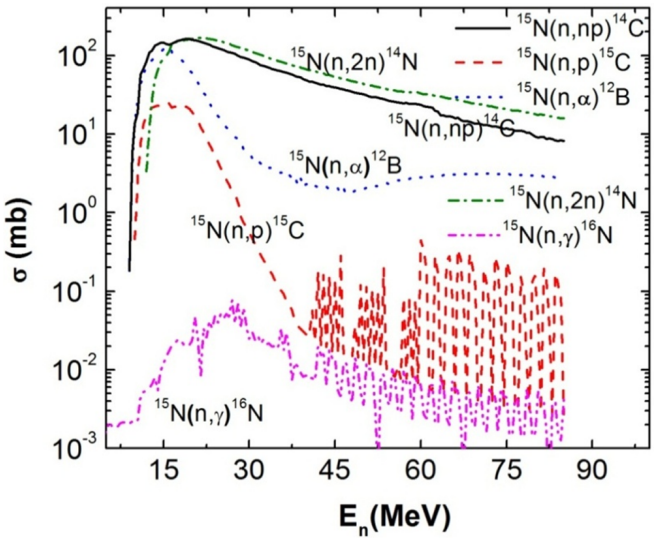

Fig. 4. (Color online) The yield of residues produced in the different channel of the n + ^{15}N reactions calculated by Talys1.4.

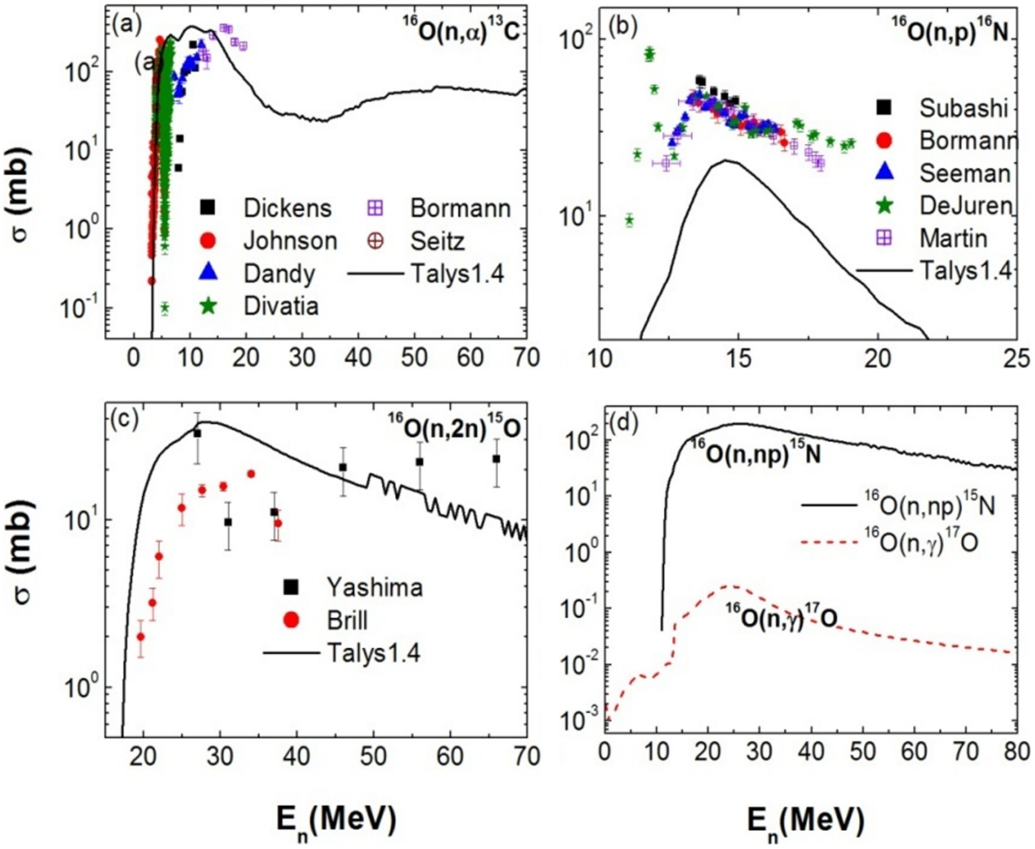

Fig. 5. (Color online) The yield of residues produced in different channels of n + ^{16}O reaction. (a) ^{16}O(n, α)^{13}C; (b) ^{16}O(n, p)^{16}N; (c) ^{16}O(n, 2n)^{15}O; and (d) ^{16}O(n, np)^{15}N and ^{16}O(n, γ)^{17}O. The results calculated by Talys1.4 are plotted as lines.

final production is the same as the ^{14}N(n, np)^{13}C channel. The ^{14}N(n, np)^{13}C channel has a low threshold energy value of about 6.00 MeV, and the cross section of the channel increase fast with E_n, which peaks at about $E_n = 14.00$ MeV.

The threshold energies increase in the order of (n, α), (n, np), and (n, 2n), which are about 0.13 MeV, 5.67 MeV and 11.27 MeV, respectively. The (n, γ) and (n, p) channel happens in the whole E_n range and forms a peak around 19.00 MeVand 9.50 MeV with a wide width, but the cross sections are very small compared to other channels.

2. $n + {}^{15}N$ reactions

No measured data for the n + ^{15}N reaction is found. Only the Talys1.4 calculated results are plotted in Fig. 4. The calculated results for the (n, np) and (n, α) channels have almost the same values when $E_n < 12.00$ MeV and the (n, np) channel has much larger values than that of the (n, α) channel. At the same time, the cross sections of (n, p) and (n, 2n) channels only have small difference when $E_n > 17.00$ MeV. The (n, np), (n, α), (n, p), and (n, 2n) channels have relatively similar threshold energy values, which are about 8.57 MeV, 8.09 MeV, 9.55 MeV and 11.56 MeV, respectively. The cross sections of the (n, γ) channel are much smaller compared to the other channels. When $E_n > 40.00$ MeV, large fluctuations are found in the results of the (n, p) and (n, γ) channels.

C. Neutron induced reactions on oxygen isotopes

The O element has three stable isotopes, ^{16}O, ^{17}O, and ^{18}O, with a natural abundance of 99.75%, 0.0038%, and 0.205%. Only the n + ^{16,18}O reactions are calculated.

1. $n + {}^{16}O$ reactions

In Fig. 5, the results of the n + ^{16}O reactions are plotted. The channels include ^{16}O(n, α)^{13}C, ^{16}O(n, p)^{16}N, ^{16}O(n, 2n)^{15}O, ^{16}O(n, np)^{15}N, and ^{16}O (n, γ) ^{17}O. ^{16}N decays to ^{16}O by emitting electron with a half-life time of 7.13 s. Thus the main channels which make the element change are ^{16}O(n, α)^{13}C and ^{16}O(n, np)^{15}N.

For the ^{16}O(n, α)^{13}C channel, the Talys1.4 calculated results are consistent with these measured by Johnson *et al.* [32], and Seitz *et al.* [33] except those by Divatia *et al.* [34] when E_n is smaller than 5.00 MeV. When $E_n > 7.00$ MeV, the measured results by Dickens *et al.* [35], Bormann *et*

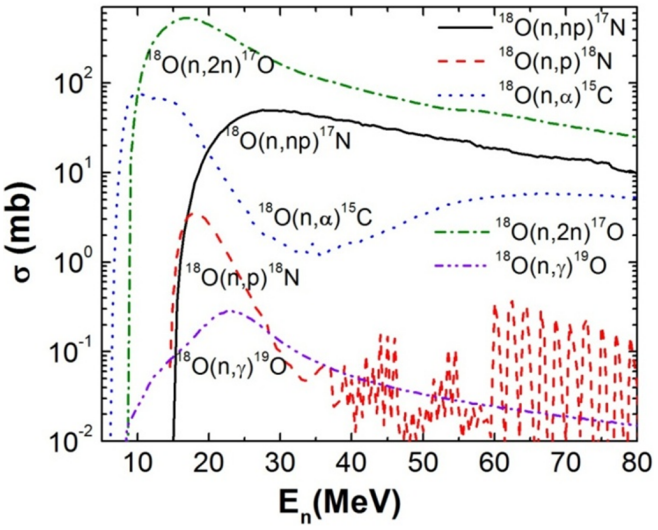

Fig. 6. (Color online) The yields of residues produced in the different channels of the n + ^{18}O reactions calculated by Talys1.4.

al. [36], and Dandy *et al*. [37] are consistent, but the Talys1.4 calculated results are unable to reproduce measured data well.

For the ^{16}O(n, p)^{16}N channel, the measured results by Martin *et al*. [38], Bormann *et al*. [39], and Seeman *et al*. [40] agree well. The measured results by Subashi *et al*. [41] and DeJuren *et al*. [42] also agree with those results but have relatively large difference. The Talys1.4 calculated results largely underestimate the measured results but have similar trend to the measured ones.

For the ^{16}O(n, 2n)^{15}O channel, the measured results by Yashima *et al*. [33] and Brill *et al*. [17] are in different energy ranges, but for the overlapping range of E_n, the results have some difference. The Talys1.4 results overestimate the measured ones when $E_n < 40.00$ MeV, but underestimate the measured ones when $E_n > 40.00$ MeV.

The ^{16}O(n, np)^{15}N and ^{16}O(n, γ)^{17}O channels have not been measured. For the ^{16}O(n, np)^{15}N channel, the probability increases fast above the threshold energy of 10.57 MeV and has a maximum value around $E_n = 20.00$ MeV. The ^{16}O(n, γ)^{17}O channel happens in the whole E_n range but have much smaller values.

The Talys1.4 calculated threshold energies of the (n, α), (n, p), (n, np) and (n, 2n) channels for ^{16}O are 2.36 MeV, 10.25 MeV, 10.57 MeV and 16.65 MeV, with peaks form at around 10.00 MeV, 14.50 MeV, 26.00 MeV and 28.00 MeV, respectively.

2. *n* + ^{18}*O reactions*

The main channels that the n + ^{18}O reactions cover are ^{18}O(n, α)^{15}C, ^{18}O(n, np)^{17}N, ^{18}O(n, p)^{18}N, ^{18}O(n, 2n)^{17}O, and ^{18}O(n, γ)^{19}O. ^{17}N can decay to ^{16}O and ^{17}O with a half-life time of 4.173 s; ^{18}N can decay to ^{18}O, ^{14}C, or ^{17}O with a half-life time of 622 ms, which are all stable nuclei (^{14}C has a very long half-life time).

In Fig. 6, the calculated results for the channels are plotted. The thresholds of the (n, α), (n, 2n), (n, p), and (n, np) channels are 5.29 MeV, 8.49 MeV, 13.85 MeV and 14.49 MeV, and the peaks form at around 10.00 MeV, 17.00 MeV, 18.00 MeV and 49.50 MeV, respectively. When $E_n > 33.00$ MeV, the yield of the (n, p) channel has large fluctuations with E_n.

D. Comparison between main channels of n + C/N/O isotopes

The differences between the threshold energies of the different channels make it possible to change one element to another. To change the element in organic materials specifically, the incident energy of the neutron should be selected to fit the energy window, as has been illustrated in the results above. The comparison between the thresholds of the main channel inducing element changes will show the E_n window more clearly.

For ^{12}C, both the final production of ^{12}C(n, np)^{11}B and ^{12}C(n, 2n)^{11}C are ^{11}B since ^{11}C decays to ^{11}B via positron emission with a half-life time of 20.30 ms. The threshold energy of ^{12}C(n, α)^{9}Be is about 6.18 MeV. When $E_n > 7.00$ MeV, ^{12}C can be changed to ^{9}Be. The threshold energy of ^{12}C(n, np)^{11}B is about 14.89 MeV. When $E_n > 16.00$ MeV, ^{12}C can be changed to ^{9}Be and ^{11}B. This provides actual application of neutron activation on C isotopes. The chemically synthesized compound, in which a C atom is substituted by a B atom, demonstrates a novel molecular engineering concept of organic semiconductors [43]. For ^{14}N, the most important channel is (n, 2n), which happens at very low neutron incident energy. Since the final yields in the n + ^{14,15}N reactions are mainly carbon isotopes, we do not discuss the energy window for these channels. For ^{16}O, the main channels are ^{16}O(n, α)^{13}C and ^{16}O(n, np)^{15}N when $E_n < 15.00$ MeV, with the production of ^{13}C and ^{15}N, respectively. There is also an E_n window between the two channels in the range from 4.00 MeV to 11.00 MeV. With larger E_n, the ^{16}O(n, 2n)^{15}O channel is opened. ^{15}O decays to ^{14}N by emitting a positron with a half-life time of 70.60 s, i.e., ^{16}O is changed to ^{14}N finally.

For a better understanding of the energy windows, the energy above the Talys calculated threshold energy for each channel is plotted in Fig. 8. The numbers from 1 to 24 represent the channels and the alphabet from a to w represent the values of the threshold energies, of which are also listed as follows (the unit is MeV): 1, $E_n = 0$ for the ^{14}N(n, p)^{14}C and (n, γ) channel of C/N/O; 2, ^{14}N(n, α)^{11}B (a = 0.13); 3, ^{16}O(n, α)^{13}C (b = 2.36); 4, ^{13}C(n, α)^{10}Be (c = 4.13); 5, ^{18}O(n, α)^{15}C(d = 5.29); 6, ^{13}C(n, 2n)^{12}C (e = 5.33); 7, ^{14}N(n, np)^{13}C (f = 5.67); 8, ^{12}C(n,α)^{9}Be (g = 6.18); 9, ^{15}N(n, α)^{12}B (h = 8.09); 10, ^{18}O(n, 2n)^{17}O (i = 8.49); 11, ^{15}N(n, np)^{14}C (j = 8.57); 12, ^{15}N(n, p)^{15}C (k = 9.55); 13, ^{16}O(n, p)^{16}N (l = 10.25); 14, ^{16}O(n, np)^{15}N (m = 10.57); 15, ^{14}N(n, 2n)^{13}N (n = 11.27); 16, ^{15}N(n, 2n)^{14}N (o = 11.56); 17, ^{13}C(n, p)^{13}B (p = 13.635); 18, ^{12}C(n, p)^{12}B (q = 13.645); 19, ^{18}O(n, p)^{18}N (r = 13.85); 20, ^{18}O(n, np)^{17}N (s = 14.49); 21, ^{12}C(n, np)^{11}B (t = 14.89); 22,

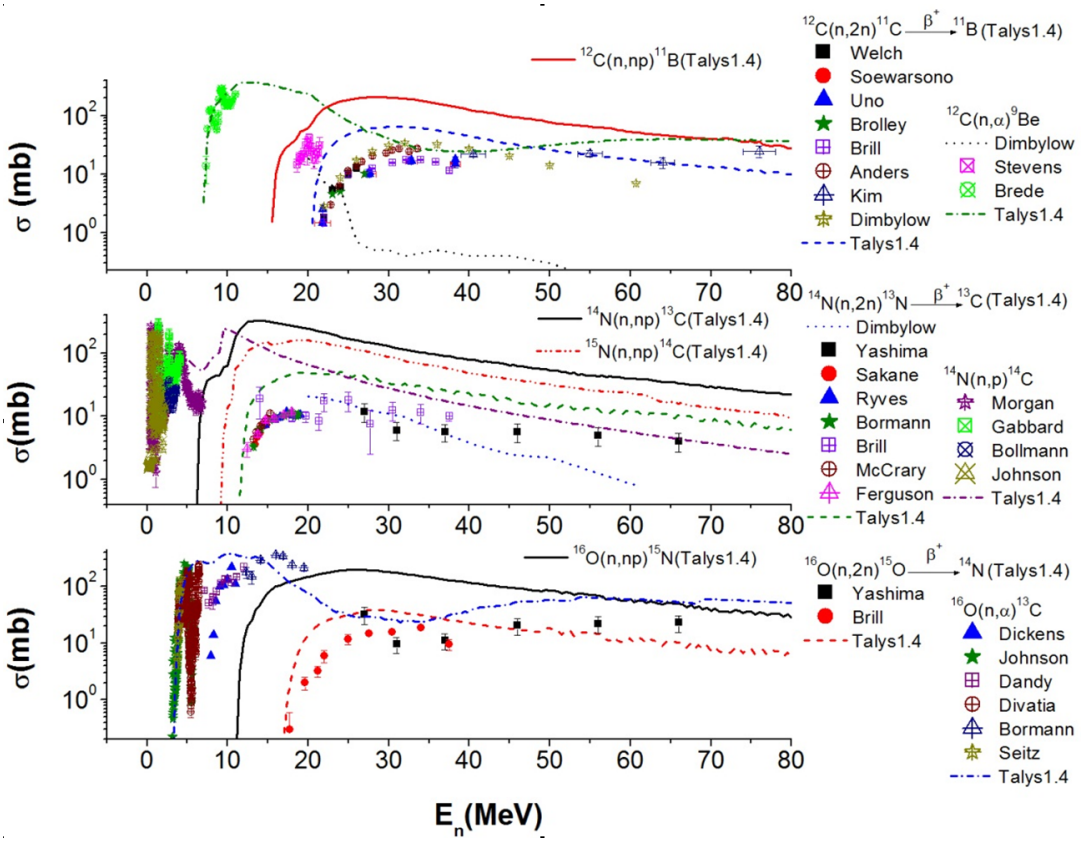

Fig. 7. (Color online) Comparison among the results of the main channels of n + C/N/O reactions which induce element changes.

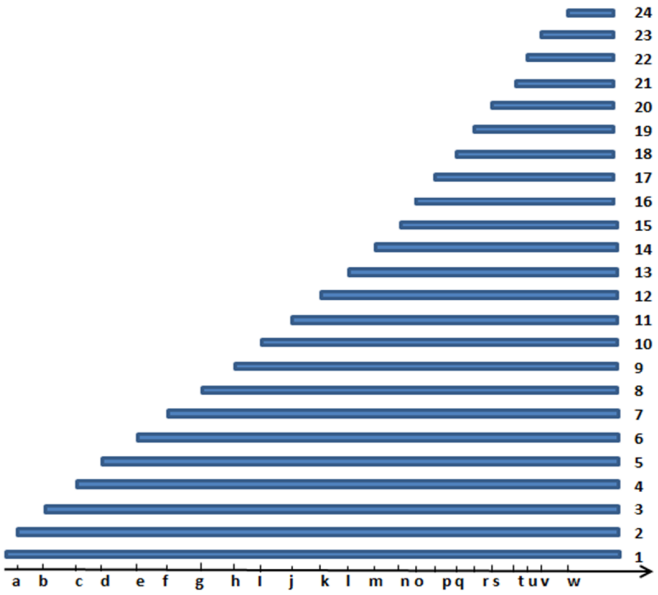

Fig. 8. (Color online) The comparison among the threshold energies of different channels which induce element changes (See the text for explanation).

^{13}C(n, np)^{12}B (u = 16.49); 23, ^{16}O(n, 2n)^{15}O (v = 16.65); 24, ^{12}C(n, 2n)^{11}C (w = 20.30). Though the energy windows are clearly shown in Fig. 8, it should be carefully analyzed when the neutron is used to activate special compounds, including different elements.

IV. CONCLUSION

In this article, the neutron induced reactions on the stable C, N, and O isotopes are investigated by using the Talys1.4 toolkit, which calculates the reactions in the framework of optical model. On the one hand, it is found that for ^{12}C and ^{14}N, the Talys1.4 results agree with the experimental data, while for ^{16}O, the parameters in Talys1.4 should be adjusted for a better prediction. On the other hand, a systematic comparison among the main channels of n + C/N/O reactions which induce element change are performed to find E_n windows among the original C, N, and O stable isotopes (by considering the final production of the channel, i.e., direct change or indirect change through decay to a different element isotope). In these E_n windows, specific elements can be activated to a different one while leaving the other element unchanged. The results may help to study material modification by using neutron induced doping techniques such as in organic materials like the organic semiconductor.

[1] Ikai M, Tokito S, *et al*. Appl Phys Lett, 2001, **79**: 156–158.
[2] Scherf U and List E J W. Adv Mater, 2002, **14**: 477–487.
[3] Ding D Z, Ye C T, Zhao Z X, *et al*. Neutron Physics. Bejing (China): Atomic Energy Publishing, 2005.
[4] Raynal J. Notes on ECIS94, CEA Saclay Report No. CEA-N-2772, 1994.
[5] Ma C W, Jing R Y, Feng X, *et al*. Chinese Phys C, 2014. (in press)
[6] Koning A J, Hilaire S, Duijvestijn M C, *et al*. User Manual of Talys-1.4. (http://www.talys.eu/_leadmin/talys/user/docs/talys1.4.pdf).
[7] https://www-nds.iaea.org/exfor/exfor.htm
[8] http://en.wikipedia.org/wiki/Isotope
[9] Brede H J, Dietze G, Klein H, *et al*. Nucl Sci Eng, 1991, **1**: 22–34.
[10] Stevens A P. INIS microfiche, No. 3596, 1976.
[11] Dimbylow P J. Phys Med Biol, 1980, **4**: 637–649.
[12] Kreger W E and Kern B D. Phys Rev, 1959, **113**: 890–894.
[13] Rimmer E M and Fisher P S. Nucl Phys A, 1968, **108**: 567–576.
[14] Welch P, Johnson J, Randers-Pehrson G, *et al*. B Am Phys Soc, 1981, **26**: 708.
[15] Anders B, Herges P, Scobel W. Z Phys A-Hadron Nucl, 1981, **4**: 353–361.
[16] Kim E, Nakamura T, Konno A, *et al*. Nucl Sci Eng, 1998, **129**: 209–223.
[17] Brill O D, Vlasov N A, Kalinin S P, *et al*. Dokl Akad Nauk+, 1961, **1**: 55.
[18] Uno Y, Uwamino Y, Soewarsono T S, *et al*. Nucl Sci Eng, 1996, **122**: 247–257.
[19] Brolley J E, Jr, Fowler J L, *et al*. Phys Rev, 1952, **88**: 618–621.
[20] Soewarsono T S, Uwamino Y, Nakamura T. JAERI-M Reports, No. 92, 027, 354, 1992.
[21] Gabbard F, Bichsel H, Bonner T W. Nucl Phys, 1959, **14**: 277–294.
[22] Khryachkov V Y, Kuzminov B D, Dunaev M V, *et al*. Atomnaya Energiya, 2006, **101**: 760–765.
[23] Morgan G L. Nucl Sci Eng, 1979, **70**: 163–176.
[24] Johnson C H and Barschall H H. Phys Rev, 1950, **80**: 818–823.
[25] Bollmann W and Zuenti W. Helve Phys Acta, 1951, **24**: 517–550.
[26] Sakane H, Kasugai Y, Shibata M, *et al*. Ann Nucl Energy, 2001, **28**: 1175–1192.
[27] Ryves T B, Kolkowski P, Zieba K J. J Phys G Nucl Partic, 1978, **4**: 1783–1792.
[28] Bormann M, Fretwurst E, Schehka P, *et al*. Nucl Phys, 1965, **63**: 438–448.
[29] Mc Crary J H and Morgan I L. B Am Phys Soc, 1960, **5**: 246.
[30] Ferguson J M and Thompson W E. Phys Rev, 1960, **118**: 228–232.
[31] Yashima H, Terunuma K, Nakamura T, *et al*. J Nucl Sci Technol, 2004, **4**: 70–73.
[32] Johnson C H, Fowler J L, Feezel R M. Oak Ridge National Lab. Reports, No. 4743, 37, 1972.
[33] Seitz J and Huber P. Helvetica Physica Acta, 1955, **28**: 227–244.
[34] Divatia A S, Sekharan K K, Mehta M K, *et al*. Nucl Data React Conf, 1966, **1**: 233.
[35] Dickens J K and Perey F G. Nucl Sci Eng, 1970, **40**: 283–293.
[36] Bormann M, Cierjacks S, Fretwurst E, *et al*. Z Phys, 1963, **174**: 1.
[37] Dandy D, Wankling J L, Parnell C J. Aldermaston Reports, No. 60/68, 1968.
[38] Martin H C. Phys Rev, 1954, **93**: 498–499.
[39] Bormann M, Dreyer F, Neuert H, *et al*. Nucl Data React Conf, 1967, **1**: 225.
[40] Seeman K W and Moore W E. Knolls Atomic Power Lab. No. 2214, 1962.
[41] Subashi M, Gueltekin E, Reyhankan I A, *et al*. Nucl Sci Eng, 2000, **135**: 260–266.
[42] DeJuren J A, Stooksbury R W, Wallis M. Phys Rev, 1962, **127**: 1229–1232.
[43] Wang X Y, Lin H R, Lei T, *et al*. Angew Chem Int Edit, 2013, **52**: 3117–3120.